Advances in Environmental Technology 1 (2020) 37-45

Advances in Environmental Technology

journal homepage: http://aet.irost.ir

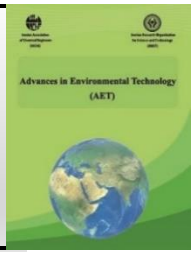

Performance of keratin nanoparticle and its magnetic nanocomposite for Zn(II) removal from its aqueous solution

Seyedeh Zahra Mousavi[a], Mehrdad Manteghian[a,*], Fatemeh Ahmadpoor[b]

[a] *Department of Chemical Engineering, Tarbiat Modares University, Tehran, Iran*

[b] *Department of Materials Engineering, Tarbiat Modares University, Tehran, Iran*

ARTICLE INFO

Article history:
Received 10 September 2020
Received in revised form
13 February 2021
Accepted 13 February 2021

Keywords:
Keratin nanoparticles
Magnetic keratin
Zn(II) removal
Adsorption isotherm
Adsorption kinetic

ABSTRACT

The comparative sorption studies were carried out to investigate the performance of keratin nanoparticles (KNPs) and magnetic KNPs (MKNPs) for Zn(II) uptake. MKNPs showed remarkably higher Zn(II) removal due to the lower keratin weight percent in its structure (8.4%). MKNPs revealed relatively uniform Zn(II) removal within pH range between 4.0 to 6.0 at the temperature of 25°C rather than KNPs. Both KNP and MKNP exhibited two-stage kinetic behavior and reached to their equilibrium adsorption capacity within 30 min. The adsorption of Zn(II) on KNPs and MKNPs followed pseudo second order kinetic model. It was found that the experimental data were best fitted to Sips or Redlich-Peterson isotherm when KNP was used as biosorbent. Unlike KNP, MKNP conformed better to Langmuir model. The maximum adsorption capacity of MKNP at two doses of 3.0 and 5.0 g/L was calculated to be 30 and 18 mg/g, respectively. As the dosage of MKNP raised from 3.0 to 5.0 g/L, the value of K_L increased from 0.045 L/mg to 0.154 L/mg, confirming more biosorbent tendency to adsorb metal ions.

1. Introduction

Heavy metals are widely used in various industrial applications. Among the heavy metals, zinc is one of the most used ones which is applied in various industries including electroplating, battery manufacturing, dying, fertilizer and pesticide, herbicides, algicides and etc. [1]. Although zinc is essential element for human, it become toxic as exceeds its tolerance level [2-4]. Hence, discharging zinc into the environment have detrimental effect on human health as well as the ecosystem. So, it is of great importance to remove it from the industrial effluents even at low concentration. Based on the regulation introduced by the environmental protection agency, the acceptable concentration of Zn(II) in the water should not exceed 5mg/L [1]. Conventional methods for heavy metal removal includes chemical precipitation, ion-exchange, adsorption, electrolysis, filtration, reverse osmosis, etc. [4-7]. Among them, adsorption using biosorbent is an innovative promising technology due to its simplicity, low operational costs and high efficiency, especially at low metal concentration [8]. Various natural low cost materials are used in the biosorption process such as chitin/chitosan [9,10], alginate [11,12], dead biomass [13], seaweed[14], etc. Recently, researchers used chicken feather for heavy metal removal as a new biosorbent [15-17]. Chicken feather is a byproduct of poultry industry and rich source of protein (keratin). The existence of various functional groups in the keratin structure makes it applicable as a biosorbent. Besides, synthesis of nano-sized biosorbent exhibit the advantage of high surface area, low diffusion resistance and more active sites. However, the drawback which coexist with the nano-sized biosorbent is their separation problem from the medium due to their high surface energy [18]. To overcome this problem, magnetic nanoadsorbents are designed. Various magnetic biomaterials were synthesized and used for heavy metal removal including L-arginine [19], chitosan [20-22], agricultural biomass [23], cellulose [24] and etc. In our previous work, we have synthesized MKNPs as a new magnetic biosorbent [25]. The main purpose of this

*Corresponding author.
Email address: manteghi@modares.ac.ir
DOI: 10.22104/AET.2021.4406.1235

research is to study and compare and the adsorption efficiency, isotherm and kinetics of Zn(II) removal using Keratin before and after its immobilization.

2. Materials and methods

2.1. KNP synthesis

KNP was synthesized based on our previous work [26]. Briefly, keratin dispersion was prepared by adding Tris (hydroxymethyl) aminomethane and optimizing its ratio to the keratin weight. Then, the mixture was stirred at 400 rpm for 16 h under room temperature to make the particles smaller. It was then sonicated (300 W, 10 min) with a probe ultrasonic device (UP400-A, the Ultrasonic Technology Development Company) to break the microparticles into nanoparticles. The synthesized KNPs could be used in form of dispersion in a liquid medium or solid powder.

2.2. MKNP preparation

Co-precipitation method was used for MKNP synthesis[25]. Briefly, ferric chloride (0.540 g) and ferrous chloride (0.199 g) with a molar ratio of 2:1 were dissolved in an aqueous KNP dispersion (0.5 g/L, 100 mL). The mixture was stirred under an argon atmosphere in a three-necked flask. Then, the ammonium hydroxide solution (7 mL) was added to the system instantaneously and the magnetic nanocomposite precipitated. MKNPs were separated using a magnet and washed several times with deionized water. The magnetic biosorbent was stored in the atmosphere of argon before use. MNKPs, KNPs and MNPs were characterized with TEM (LEO 906, 80 kV). For TEM imaging, KNPs were negatively stained. Then, all three nanoparticle samples were sonicated for 3 min. Then, a drop of the sample was placed on a carbon copper grid, dried at room temperature, and observed under TEM.

2.3. Batch adsorption experiments

The stock solution (1000 mg/L) of Zn(II) was prepared by zinc chloride salt. The optimum biosorbent dosage was determined by adding different doses of biosorbent (0.1-7.0 g/L) to the heavy metal solution of 100 mg/L. The samples were shaken for 30 min to reach the equilibrium. MKNPs could be separated by applying external magnetic field after Zn(II) adsorption. Because KNPs precipitate after metal adsorption they were conveniently separated by centrifugation at 1000×g for 5 min. For further adsorption experiments, the obtained optimum biosorbent dosage, based on the maximum heavy metal removal, was used. The influence of solution pH on MKNP efficiency was investigated in the range of 4.0-6.0 (adjusted with HCl or NaOH solution). To avoid Zn(II) precipitation due to the formation of zinc hydroxide, the experiments were performed at pH values lower than 6.0. Hence, metal precipitation does not interfere with biosorbent function. When using KNP as the biosorbent, the value of pH restricted in the range of 5-6 to prevent KNP precipitation. All the experiments were done at an ambient temperature of 25°C. The residual metal concentration was measured using a flame *atomic absorption spectrophotometer* (*Shimadzu AA-670*).

2.4. Adsorption kinetics

The heavy metal concentration was measured at different time intervals to study the adsorption kinetics. The experiments were done at the heavy metal initial concentration of 100 mg/L and pH value of 6.0. The pseudo-first [27] and pseudo-second order [28] rate equations were applied to model the kinetics of Zn(II) adsorption. These models are represented in Equations (1-2):

$$\ln(q_e - q_t) = \ln q_e - k_1 t \quad (1)$$

$$\frac{t}{q_t} = \frac{1}{k_2 q_e^2} + \frac{1}{q_e} t \quad (2)$$

where q_e and q_t (mg/g) are the adsorption capacities at equilibrium and time t; k_1 (min^{-1}) and k_2 (g mg^{-1} min^{-1}) are pseudo-first order and pseudo-second order rate constants.

2.5. Adsorption isotherm

The heavy metal stock solution was diluted in the range of 40-400 mg/L to study the adsorption isotherm at an ambient temperature of 25 °C and pH value of 6.0. The equations (3) and (4) could be applied to calculate the adsorption capacity at the equilibrium and the removal efficiency of heavy metal, respectively [29].

$$q_e = \frac{V(C_0 - C_e)}{m} \quad (3)$$

$$R(\%) = \frac{C_0 - C_e}{C_0} \times 100 \quad (4)$$

where C_0 and C_e (mg/L) are the initial and equilibrium concentrations of the heavy metal, V (L) is the volume of the solution, and m (g) is the mass of the biosorbent. The interaction of the heavy metal with the biosorbent could be characterized with the adsorption isotherm models. The two parameter adsorption isotherm models of Langmuir and Freundlich, as well as the three parameter models of Sips and Redlich-Peterson, were employed to study the metal uptake as a function of its equilibrium concentration using CurveExpert software [30].

2.5.1. Langmuir adsorption isotherm

Langmuir adsorption model is represented by the following equation [31]:

$$q_e = \frac{K_L q_m C_e}{1 + K_L C_e} \quad (5)$$

where q_e is the amount of metal adsorbed per unit mass of biosorbent (mg/g), C_e refers to the residual metal at the equilibrium (mg/L), K_L is Langmuir constant or the energy of adsorption (L/g), and q_m denotes the maximum adsorption capacity of the biosorbent (mg/g). Separation factor (R_L) is a dimensionless parameter which is used to predict the

favorability of the adsorption process. It can be expressed as:

$$R_L = \frac{1}{1 + K_L C_0} \quad (6)$$

where C_0 denotes the initial metal concentration (mg/L). The value of R_L indicates whether the adsorption is unfavorable (R_L>1), linear (R_L=1), favorable (0<R_L<1) or irreversible (R_L=0).

2.5.2. Freundlich adsorption isotherm

The Freundlich isotherm is an empirical model which can be expressed by the following equation [32]:

$$q_e = K_F C_e{}^{1/n} \quad (7)$$

where K_F (mg/g) and n are the Freundlich constants related to the adsorption capacity and intensity, respectively.

2.5.2. Redlich-Peterson adsorption isotherm

The Redlich-Peterson isotherm is an empirical three parameter model combining the features of both Langmuir and Freundlich isotherms. This model is applicable in both homogeneous and heterogeneous systems and can be represented as [33]:

$$q_e = \frac{K_{RP} C_e}{1 + a_{RP} C_e{}^{\beta_{RP}}} \quad (8)$$

where K_{RP} (L/mg), a_{RP} and β_{RP} are Redlich-Peterson constants. When the concentration is high, the value of $a_{RP} C_e{}^{\beta_{RP}}$ is much bigger than unity (β_{RP} tends to zero) and the isotherm reduces to the Freundlich model. It also reduces to Langmuir isotherm in the cases of low metal concentrations (β_{RP} approaches to 1). The ratio of K_S/a_S represents the adsorption monolayer capacity [34,35].

2.5.3. Sips adsorption isotherm

The Sips equation includes three parameters and is a combination of Langmuir and Freundlich isotherms deducted for the heterogeneous adsorption systems. It can be expressed as [36]:

$$q_e = \frac{K_S C_e{}^{\beta s}}{1 + a_S C_e{}^{\beta s}} \quad (9)$$

where K_S (L/mg), a_S and β_S are Sips constants. The equation approaches to Langmuir isotherm at high adsorbate concentration, and it reduces to the Freundlich isotherm at low adsorbate concentration. The operation conditions such as solution pH, temperature and concentration govern the parameters of Sips equation.

2.6. Statistical analysis

All the experiments were carried out in duplicate or triplicate and the reported data are mean values ± standard deviation (SD). SD was calculated based on the standard equations and the error bars are shown wherever needed.

3. Results and discussion

3.1. Morphology of NPs

The TEM image of MNPs, KNPs, and MKNPs are shown in Figure 1. As it can be seen in Figure 1a, MNPs are almost spherical. As it is indicated in our previous work, MNPs have a mean size of 12.4±2.2 nm [25]. KNPs also seems to be spherical (Figure 1b). However, the nanoparticles were agglomerated after drying. These particles have a mean size of about 33nm [26]. After synthesis of MKNPs, MNPs were coated with keratin and they have a core-shell structure (Figure 1c). These particles have a mean size of 15.0±3.5 nm [25].

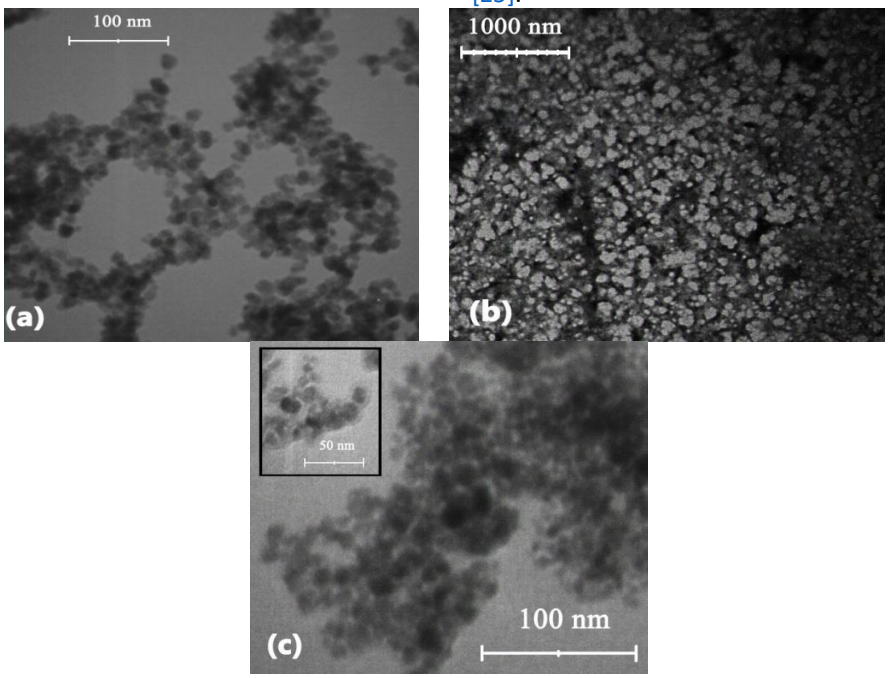

Fig. 1. TEM image of (a) MNPs, (b) KNPs, after negative staining, and (c) MKNPs; as it can be seen MKNPs have a core-shell structure.

3.2. Effect of biosorbent dosage

The experiments to investigate the dependence of biosorbent dosage on Zn(II) removal were done at biosorbent dosage in the range of 0.1-7.0 g/L, while other parameters were kept constant. As it can be seen in Figure 2, at lower KNP doses (0.1-3.0 g/L), Zn(II) removal increases with increasing KNP dosage. It can be attributed to the large number of strong affinity binding sites for Zn(II) removal. However, there is a critical dosage (3.0 g/L) that beyond it KNPs become so close to each other that are aggregated easily due to their inter-particle interactions. It might lead to the decrease of the biosorbent adsorption sites as well as the removal percentage. So, KNP dosage of 3.0 g/L was selected as the optimum dosage. Using MKNP as a biosorbent, the removal efficiency increases up to 98% by increasing the biosorbent dosage (0.1-5.0 g/L). Any further increase in MKNP dosage (beyond 5.0 g/L) does not have much effect on Zn(II) removal due to the saturation of the adsorption sites. The reason of this trend might be due to the presence of the low keratin weight percent in MKNP structure (8.4%) which decreases the probability of overcrowding and aggregation of the biosorbent particles [25]. So, MKNP concentration of 5.0 g/L was selected as the optimum dosage.

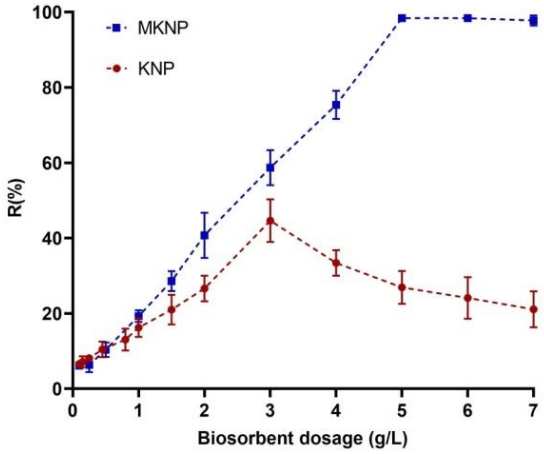

Fig. 2. The effect of biosorbent dosage on Zn(II) removal using KNP and MKNP at Zn(II) concentration of 100 mg/L, and T=25 °C. The bars represent the standard deviation (n=2).

3.3. Effect of initial solution pH

In order to investigate the effect of initial solution pH on MKNP performance, a number of experiments were done at pH range of 4.0-6.0 while the other parameters were kept constant (MKNP dosage of 1.5 g/L and Zn(II) concentration of 100 mg/L). The pH values higher than 6.0 were not examined due to Zn(II) precipitation that might interfere with biosorbent function. As it is shown in Figure 3, Zn(II) removal is relatively constant in this range, indicating MKNP can be used in pH range of real applications. This might be attributed to the deprotonation of amino and carboxylic groups[37]. Using KNP as biosorbent, all the adsorption experiments were done at the pH value of about 5. Because the isoelectric point of keratin (at the pH value of about 4.4) and Zn(II) precipitation (at pH values higher than 6.0) were two restrictive factors.

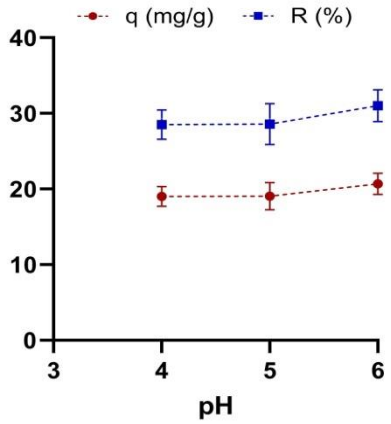

Fig. 3. The effect of initial solution pH on adsorption capacity and removal of Zn(II) using MKNP. The bars represent the standard deviation (n=3).

The effect of contact time on the adsorption capacity of KNP and MKNP was investigated at time intervals of 0.5, 5, 15, 30, 60 and 120 min. As it can be seen in Figure 4, the equilibrium is achieved after approximately 30 min. The achieved equilibrium adsorption capacity using KNP is lower than MKNP. It might be attributed to the existence of lower weight fraction of keratin per gram of adsorbent, resulting in decreasing aggregation probability of MKNPs in comparison to KNP. As it can be observed in Figure 4, At the beginning of the adsorption process, a rapid adsorption occurs due to the large concentration gradient between Zn(II) and biosorbent surface. Furthermore, about 80% and 90% of Zn(II) equilibrium adsorption capacities are accomplished within 30 s when using MKNP and KNP biosorbents, respectively. It can confirm the absence of internal diffusion resistance which is due to the nano-sized biosorbent particles [38].

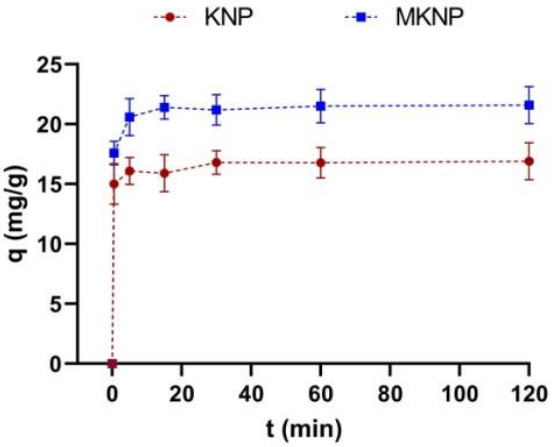

Fig. 4. The effect of contact time on the adsorption capacity of KNP and MKNP at Zn(II) concentration of 100 mg/L, and T=25 °C. The error bars represent the standard deviation (n=2).

3.5. Kinetic studies

The two commonly used adsorption kinetic models, pseudo-first order and pseudo-second order, were used to analyze Zn(II) uptake by KNP and MKNP. Plotting $ln(q_e-q_t)$ versus t according to Eq(1), the rate constant k_1 (the slope) and the equilibrium adsorption capacity q_e (the intercept) of the pseudo-first order kinetic model were calculated. The parameters are reported in Table 1. The low correlation coefficient R^2 suggests that the pseudo-first order kinetic model is not appropriate relationship to interpret Zn(II) adsorption using KNP and MKNP. Furthermore, there is a considerable difference between the calculated ($q_{e,cal}$) and the experimental ($q_{e,exp}$) adsorption capacity. Based on Eq(2), by plotting t/q_t versus t, the rate constant k_2 and the equilibrium adsorption capacity q_e of the pseudo-first order kinetic model can be calculated (Figure 5). As it can be observed in Table 1, the correlation coefficient R^2 reveals that this model is best fitted to the experimental data. The good agreement between $q_{e,cal}$ and $q_{e,exp}$ also confirms that Zn(II) biosorption using both KNP and MKNP follows pseudo-second order kinetic model and it follows a chemisorption process.

Table 1. The parameters of adsorption kinetic models for Zn(II) adsorption on KNP and MKNP

Model	Parameters	KNP	MKNP
Pseudo-first order model	$q_{e,exp}$ (mg/g)	16.9	21.6
	$q_{e,cal}$ (mg/g)	2.7	3.2
	$k_1\times10^3$ (min^{-1})	6.6	6.7
	R^2	0.64	0.61
Pseudo-first order model	$q_{e,cal}$ (mg/g)	16.9	21.7
	k_2 ($g.mg^{-1}min^{-1}$)	0.15	0.17
	R^2	1.0	1.0

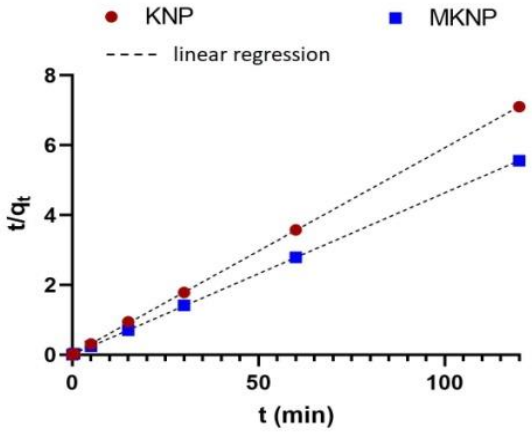

Fig. 5. Pseudo second order kinetic fits for Zn(II) adsorption on KNP and MKNP.

3.6. Equilibrium isotherm models

The non-linear form of Langmuir, Freundlich, Sips and Redlich-Peterson were used to analyze the interaction of Zn(II) with the biosorbent and the adsorption efficiency. The results of fitting the experimental data with the Langmuir and Freundlich isotherms are presented in Table 2. The correlation coefficients suggest that the deviation of the experimental data from Freundlich model becomes more as the biosorbent dosage increases. Furthermore, changing the biosorbent from KNP to MKNP results in more deviation from Freundlich model. The Langmuir model assumes the monolayer adsorption with homogeneous distribution over the surface containing finite number of identical binding sites [39]. The calculated Langmuir parameters are presented in Table 2. As it can be seen, the value of q_m decreases by switching the biosorbent from KNP to MKNP which can be attributed to the presence of lower weight percent of keratin in the structure of MKNP rather than KNP. As it can be seen in Table 2, the value of q_m decreases as the adsorbent dosage increases. It is predicted that this happens due to the high aggregation tendency of Keratin. At the lower biosorbent doses, the probability of the aggregation is lower and the maximum adsorption capacity is higher. However, at the higher adsorbent doses, the number of the surface bonding sites increases and the probability of the aggregation becomes higher. So, the available sites forZn(II) removal decreases as well as the maximum adsorption capacity. The value of K_L is higher when using MKNP, which indicates the higher energy of adsorption.

Zn(II) uptake using both KNP and MKNP is favorable process, since R_L ranged between 0 and 1. Finally, considering the correlation coefficient, it can be concluded that the experimental data of Zn(II) uptake using MKNP are well fitted to Langmuir model. The results of fitting the experimental data with the three-parameter models of Sips and RP are presented in Table 3. Based on the correlation coefficients, the adsorption process is well defined by both models. When the exponent β_S is almost 1.0, the Sips equation reduces to Langmuir equation. Thus, it is expected that the maximum adsorption capacity of each layer (K_S/a_S) be almost the same as the maximum adsorption capacity of Langmuir [34]. As it can be seen in Table 3, at MKNP dosage of 5.0 g/L these values are very close to each other. The deviation of the value of β_S from unity indicates heterogeneous surface [40,41]. When fitting RP isotherm with the adsorption data, the exponent β_{RP} should be in the range of 0-1.0 [42].The value of β_{RP} at MKNP dosage of 5.0 g/L is exactly 1.0, indicating that this model reduces to Langmuir [35]. The correlation coefficient also confirms it. Figure 6 shows the best fitted isotherm of each sample.

Table 2. Freundlich and Langmuir isotherm constants for Zn(II) adsorption on KNP and MKNP

Biosorbent	Dosage (g/L)	Freundlich model			Langmuir model				
		K_F (mg/g) (mg/L)^n	n	R^2	q_m (mg/g)	$K_L \times 10^3$ (L/mg)	R_L C_0 = 40 (mg/L)	R_L C_0 = 400 (mg/L)	R^2
KNP	1.5	0.5	1.3	0.92	73	3.0	0.46	0.89	0.73
	3.0	0.9	1.6	0.88	38	7.6	0.25	0.77	0.94
MKNP	3.0	14.5	9.6	0.87	30	54.7	0.04	0.31	0.96
	5.0	11.6	12.3	0.67	18	153.7	0.02	0.14	0.99

Table 3. Redlich-Peterson and Sips isotherm constants for Zn(II) adsorption on KNP and MKNP

Biosorbent	Dosage (g/L)	Redlich-Peterson model				Sips model				
		K_{RP}	a_{RP}	β_{RP}	R^2	K_S/a_S	K_S	β_S	a_S	R^2
KNP	1.5	0.29	0.02	0.78	0.98	70	0.30	0.95	4.31×10^{-3}	0.98
	3.0	0.31	4.29×10^{-3}	1.12	0.98	27	0.05	1.56	1.68×10^{-3}	0.98
MKNP	3.0	2.31×10^{9}	1.69×10^{-8}	0.88	0.90	-	4.37×10^{-3}	2.94×10^{-5}	-1.00	0.93
	5.0	101.86	6.01	1.00	0.93	17	101.03	1.01	5.89	0.93

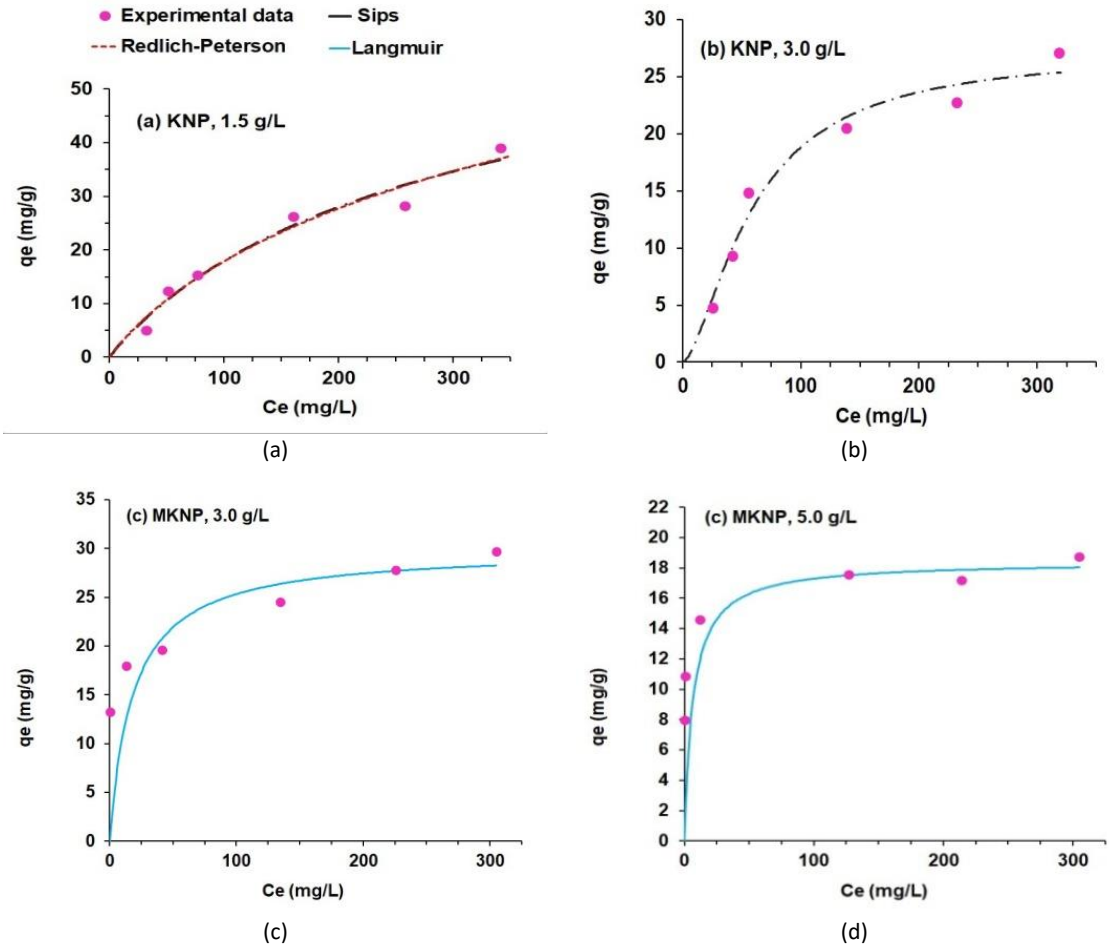

Fig. 6. The best fitted adsorption isotherms: (a) Sips and RP for Zn(II) biosorption on KNP, dosage of 1.5 g/L; (b) Sips for Zn(II) biosorption on KNP, dosage of 3.0 g/L; and Langmuir for Zn(II) biosorption on MKNP at dosage of (c) 3.0 g/L and (d) 5.0 g/L.

3.7. Comparison of MKNP constituent adsorption

The Removal of Zn(II) using MKNP constituents was studied at two different adsorbent doses. The main objective was to find the most important constituent for heavy metal removal as well as investigating the effect of magnetic nanoparticles (MNPs). The results are shown in Figure 7. As it can be seen in Figure 7, doubling the dosage of MNPs does not have significant effect on its removal efficiency. Besides, MNPs have the least removal compared with KNPs and MKNPs. However, the removal efficiency of KNP and MKNP increased up to twice by doubling the dosage of KNP and MKNP. It can confirm that keratin is the most important constituent for MKNP adsorption capability.

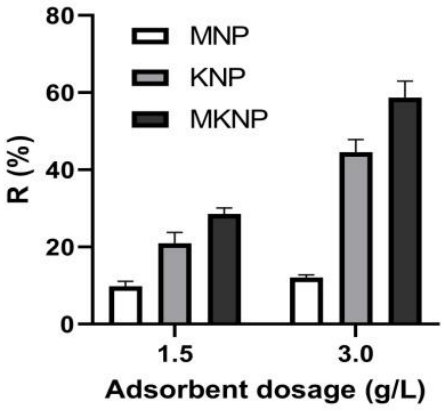

Fig. 7. Comparison of the adsorption efficiency of MKNP and its constituents (MNP and KNP) at two different sorbent dosage of 1.5 and 3.0 g/L. The bars represent the standard deviation (n=2)

4. Conclusions

In this paper, Zn(II) uptake using KNPs and MKNPs has been investigated. Although keratin has considerable ability of Zn(II) removal, its nanocomposite with iron oxide has better performance of heavy metal removal due to lower aggregation probability as well as easy separation by applying external magnetic field. The results show that MKNPs have almost steady adsorption of Zn(II) in the pH range of 4-6, indicating its efficiency in real applications. Based on the kinetic data, both KNPs and MKNPs follow the pseudo second order kinetic model indicating the adsorption as a chemisorption process. It was observed that as the biosorbent changes from KNP to MKNP, the adsorption isotherm varies from Sips or RP to Langmuir. Hence, it can be concluded that MKNP has more homogeneous surface, with uniform energy distribution of adsorption sites. However, the fitted RP or Sips isotherms when using KNP reveals that its structure is heterogeneous and there is an interaction between adsorption layers. So, it might be concluded that the keratin has better function as a biosorbent after nanocomposite synthesis. However, this high performance of MKNP is mostly related to keratin rather than MNPs and keratin is the most important constituent for MKNP adsorption capability.

References

[1] Guidelines for drinking-water quality (2004). Vol. 1. World Health Organization.

[2] Fu, F., Wang, Q. (2011). Removal of heavy metal ions from wastewaters: a review. *Journal of environmental management*, *92*(3), 407-418.

[3] Wu, L., Zhang, X., Chen, L., Zhang, H., Li, C., Lv, Y., Guo, X. (2018). Amphoteric starch derivatives as reusable flocculant for heavy-metal removal. *RSC advances*, *8*(3), 1274-1280.

[4] Carolin, C. F., Kumar, P. S., Saravanan, A., Joshiba, G. J., Naushad, M. (2017). Efficient techniques for the removal of toxic heavy metals from aquatic environment: A review. *Journal of environmental chemical engineering*, *5*(3), 2782-2799.

[5] Ozaki, H., Sharma, K., Saktaywin, W. (2002). Performance of an ultra-low-pressure reverse osmosis membrane (ULPROM) for separating heavy metal: effects of interference parameters. *Desalination*, *144*(1-3), 287-294.

[6] Calvo, B., L. Canoira, F. Morante, J.M. Martínez-Bedia, C. Vinagre, J.-E. García-González, J. Elsen, and R. Alcantara (2009) Continuous elimination of Pb2+, Cu2+, Zn2+, H+ and NH4+ from acidic waters by ionic exchange on natural zeolites. *Journal of hazardous materials*. *166*(2-3), 619-627.

[7] Matlock, M.M., B.S. Howerton, and D.A. Atwood (2002) Chemical precipitation of heavy metals from acid mine drainage. *Water research*. *36*(19), 4757-4764.

[8] Wang, J. and C. Chen (2006) Biosorption of heavy metals by Saccharomyces cerevisiae: a review. *Biotechnology advances*. 24(5), 427-451.

[9] Ozaki, H., Sharma, K., Saktaywin, W. (2002). Performance of an ultra-low-pressure reverse osmosis membrane (ULPROM) for separating heavy metal: effects of interference parameters. *Desalination*, *144*(1-3), 287-294.

[10] Chang, Y.-C. and D.-H. Chen (2005) Preparation and adsorption properties of monodisperse chitosan-bound Fe_3O_4 magnetic nanoparticles for removal of Cu (II) ions. *Journal of colloid and interface science*. *283*(2).446-451.

[11] Deze, E.G., S.K. Papageorgiou, E.P. Favvas, and F.K. Katsaros (2012) Porous alginate aerogel beads for effective and rapid heavy metal sorption from aqueous solutions: Effect of porosity in Cu^{2+} and Cd^{2+} ion sorption. *Chemical engineering journal*. *209*, 537-546.

[12] Lagoa, R. and J.R. Rodrigues (2009) Kinetic analysis of metal uptake by dry and gel alginate particles. *Biochemical engineering journal*. *46*(3), 320-326.

[13] Das, D., G. Basak, V. Lakshmi, and N. Das (2012) Kinetics and equilibrium studies on removal of zinc (II) by untreated and anionic surfactant treated dead biomass of yeast: Batch and column mode. *Biochemical engineering journal*. *64*, 30-47.

[14] Davis, T., B. Volesky, and R. Vieira (2000) Sargassum seaweed as biosorbent for heavy metals. Water research. *34*(17), 4270-4278.

[15] Aguayo-Villarreal, I.A., A. Bonilla-Petriciolet, V. Hernández-Montoya, M.A. Montes-Moránc, and H.E. Reynel-Avila (2011) Batch and column studies of Zn^{2+} removal from aqueous solution using chicken feathers as sorbents. Chemical engineering journal. *167*, 67-76.

[16] Al-Asheh, S., F. Banat, and D. Al-Rousan (2003) Beneficial reuse of chicken feathers in removal of heavy metals from wastewater. Journal of cleaner production. *11*, 321-326.

[17] Gao, P., Z. Liu, X. Wu, Z. Cao, Y. Zhuang, W. Sun, G. Xue, and M. Zhou (2014) Biosorption of Chromium (VI) Ions by Deposits Produced from Chicken Feathers after Soluble Keratin Extraction. Clean–soil, air, water. *42*(11), 1558-1566.

[18] Wu, N., H. Wei, and L. Zhang (2011) Efficient removal of heavy metal ions with biopolymer template synthesized mesoporous titania beads of hundreds of micrometers size. Environmental science and technology. *46*(1), 419-425.

[19] Guo, S., P. Jiao, Z. Dan, N. Duan, G. Chen, and J. Zhang (2017) Preparation of L-arginine modified magnetic adsorbent by one-step method for removal of Zn (Ⅱ) and Cd (Ⅱ) from aqueous solution. Chemical engineering journal. *317*, 999-1011.

[20] Zhou, L., Y. Wang, Z. Liu, and Q. Huang (2006) Carboxymethyl chitosan-Fe_3O_4 nanoparticles: preparation and adsorption behavior toward Zn^{2+} ions. Acta Physico-Chimica Sinica. *22*(11), 1342-1346.

[21] Zhou, Y.-T., H.-L. Nie, C. Branford-White, Z.-Y. He, and L.-M. Zhu (2009) Removal of Cu^{2+} from aqueous solution by chitosan-coated magnetic nanoparticles modified with α-ketoglutaric acid. Journal of colloid and interface science. *330*(1), 29-37.

[22] Ayub, A., Z.A. Raza, M.I. Majeed, M.R. Tariq, and A. Irfan (2020) Development of sustainable magnetic chitosan biosorbent beads for kinetic remediation of arsenic contaminated water. International journal of biological macromolecules. *163*, 603-617.

[23] Noor, N.M., R. Othman, N. Mubarak, and E.C. Abdullah (2017) Agricultural biomass-derived magnetic adsorbents: Preparation and application for heavy metals removal. Journal of the Taiwan institute of chemical engineers. *78*, 168-177.

[24] Luo, X., J. Zeng, S. Liu, and L. Zhang (2015) An effective and recyclable adsorbent for the removal of heavy metal ions from aqueous system: magnetic chitosan/cellulose microspheres. Bioresource technology. *194*, 403-406.

[25] Mousavi, S.Z., M. Manteghian, S.A. Shojaosadati, and H. Pahlavanzadeh (2018) Preparation and characterization of magnetic keratin nanocomposite. Materials Chemistry and Physics. *215*, 40-45.

[26] Mousavi, S. Z., Manteghian, M., Shojaosadati, S. A., Pahlavanzadeh, H. (2018). Keratin nanoparticles: synthesis and application for Cu (II) removal. *Advances in environmental technology*, *4*(2), 83-93.

[27] Lagergren, S. (1898) Zur theorie der sogenannten adsorption geloster stoffe. Kungliga svenska vetenskapsakademiens. Handlingar. *24*,1-39.

[28] Ho, Y.-S., G. McKay (1999) Pseudo-second order model for sorption processes. Process biochemistry. *34(*5), 451-465.

[29] Khosa, M.A., A. Ullah (2014) In-situ modification, regeneration, and application of keratin biopolymer for arsenic removal. Journal of hazardous materials. *248*, 360-371.

[30] Hyams, D. (2010) CurveExpert software. URL http://www.curveexpert.net.

[31] Langmuir, I. (1916) The constitution and fundamental properties of solids and liquids. Part I. Solids. Journal of the American chemical society. *38*(11), 2221-2295.

[32] Freundlich, U. (1906) Die adsorption in lusungen.

[33] Redlich, O., D.L. Peterson (1959) A useful adsorption isotherm. Journal of physical chemistry. *63*(6), 1024-1024.

[34] Foo, K.Y. and B.H. Hameed (2010) Insights into the modeling of adsorption isotherm systems. Chemical engineering journal. *156*(1), 2-10.

[35] Al-Ghouti, M. A., Da'ana, D. A. (2020). Guidelines for the use and interpretation of adsorption isotherm models: A review. *Journal of hazardous materials*, *393*, 122383.

[36] Sips, R. (1948). On the structure of a catalyst surface. *The journal of chemical physics*, *16*(5), 490-495.

[37] Pan, L., Z. Wang, Q. Yang, and R. Huang (2018) Efficient removal of lead, copper and cadmium ions from water by a porous calcium alginate/graphene oxide composite aerogel. Nanomaterials. *8*(11), 957.

[38] Badruddoza, A., A. Tay, P. Tan, K. Hidajat, and M. Uddin (2011) Carboxymethyl-β-cyclodextrin conjugated magnetic nanoparticles as nano-adsorbents for removal of copper ions: synthesis and adsorption studies. Journal of hazardous materials. *185*(2-3), 1177-1186.

[39] Latour, R.A. (2015) The Langmuir isotherm: a commonly applied but misleading approach for the analysis of protein adsorption behavior. Journal of biomedical materials research part A. *103*(3), 949-958.

[40] Kumar, K.V. and S. Sivanesan (2006) Equilibrium data, isotherm parameters and process design for partial and complete isotherm of methylene blue onto activated carbon. Journal of hazardous materials. *134*(1-3), 237-244.

[41] Nethaji, S., A. Sivasamy, and A. Mandal (2013) Adsorption isotherms, kinetics and mechanism for the adsorption of cationic and anionic dyes onto carbonaceous particles prepared from Juglans regia

shell biomass. International journal of environmental science and technology. *10*(2), 231-242.

[42] Tran, H.N., S.-J. You, A. Hosseini-Bandegharaei, and H.-P. Chao (2017) Mistakes and inconsistencies regarding adsorption of contaminants from aqueous solutions: a critical review. Water research. *120*, 88-116.